# Supporting Information

# Nanoplasmon-Enhanced Drop-Screen for High Throughput Single-Cell Nucleocytoplasmic miRNA Profiling

Jia Liu[a,b], Guoyun Sun[a], Shih-Chung Wei[a], Song Guo[a], Weikang Nicholas Lin[a] and Chia-Hung Chen[c]*

a. Department of Biomedical Engineering, National University of Singapore, 4 Engineering Drive 3, #04-08, 117583 Singapore

b. School of Chemistry and Chemical Engineering, Nanjing University, 163 Xianlin Avenue, Nanjing, 210023, China

c. Department of Biomedical Engineering, City University of Hong Kong, 83 Tat Chee Avenue, Kowloon Tong, Hong Kong SAR, China

*E-mail: chiachen@cityu.edu.hk

Content:

**Supporting information 1. Device fabrication:**

The chip used was fabricated in polydimethylsiloxane (PDMS) using soft lithography. First, PDMS was cast on an SU-8 negative photoresist (SU-8-2050, MicroChem Inc., Newton, MA) master mold (MicroChem Inc., Newton, MA), and the thickness of the SU-8 mold of the chip was 40 μm. Second, a mixture of PDMS curing agent and prepolymer (1:10) was degassed under vacuum for approximately 1 hour and then poured onto the SU-8 model. The model was polymerized in an oven at 65 °C for at least 6 hours, and then the PDMS layer was taken from the model. Third, holes were punched through the end of the channels using a Harris Uni-Core punch with a diameter of 1.00 mm (Ted Pella, USA). Then, the PDMS chip was plasma bonded onto a PDMS-coated glass slide for increased bonding strength. The chip design is attached in Fig. S1.

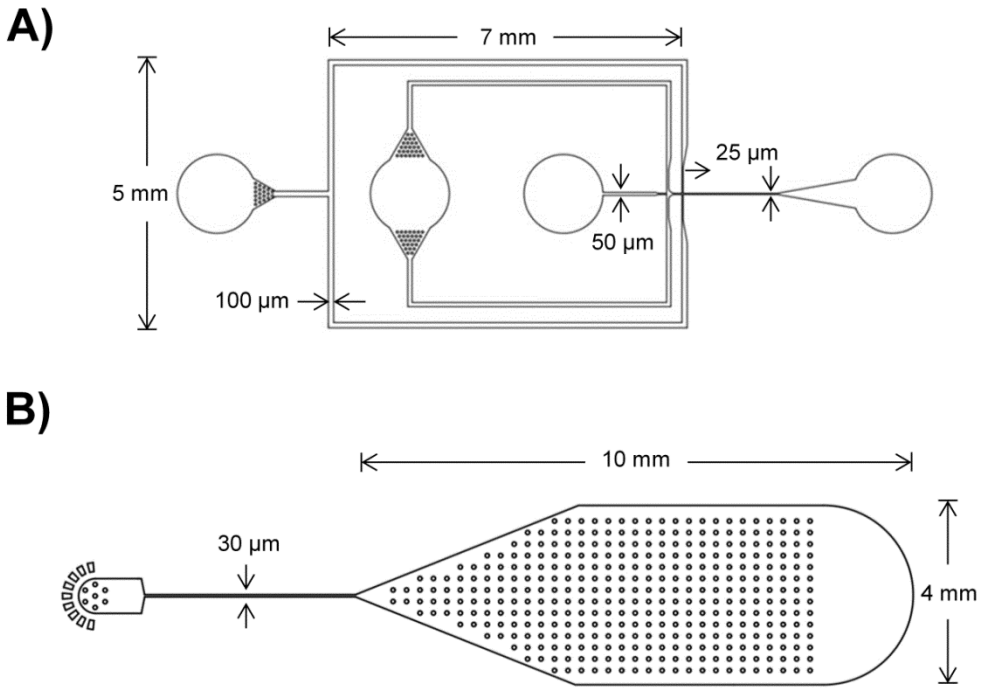


**Figure S1** Microchip used in this assay. (A) Chip used to encapsulate cells and perform PMT high-throughput screening. (B) Chip used to investigate and obtain fluorescent images of individual cells in droplets.

**Supporting information 2. Nucleus/cytoplasm-specific lysis buffer:**

Triton X-100, sodium dodecyl sulfate (SDS), tris-EDTA buffer solution (pH 8.0) and NaCl were used to prepare the nucleocytoplasmic cell lysis buffer. All these reagents were from Sigma-Aldrich (USA). The modified nucleus- and cytoplasm-specific lysis buffers were established according to a previous publication.[1,2] The cytoplasm-specific lysis buffer contains a nonionic detergent (Triton X-100) that presents a bulky head group that solubilizes the cell membrane but does not disrupt the nuclear lamina structure (formed by protein-protein interactions), thus leaving the nucleus intact. The nucleus-specific lysis buffer contains an anionic detergent (SDS) that disrupts the nucleus and solubilizes nuclear proteins (Table S1).

It is worth noting that there are two factors to prevent AgNP dimer degradation. Firstly, the lysis buffer used contains Ethylene Diamine Tetraacetic Acid (EDTA), enabling suppress enzyme activities to prevent degradation of nucleic acids in AgNP dimers. Moreover, NaCl in the lysis buffer is conducted to stabilize nucleic acid structure.[3,4] Secondly, the droplet with cell lysis was kept at low temperature (~0 °C) to ensure the stability of AgNP dimers (sequence between AgNPs is integrity) when measuring target miRNA.

**Table S1** Formulation of nucleus/cytoplasm-specific lysis buffer.

| Reagents | Cytoplasm-specific buffer | Nucleus-specific buffer |
|---|---|---|
| Triton X-100 | 1% (v/v) | - |
| SDS | - | 10 mg/mL |
| NaCl | 50 mM | 50 mM |
| EDTA | 2 mM | 2 mM |
| Tris | 20 mM | 20 mM |

(pH: 7.6)

**Supporting information 3. Sequences used to fabricate the nanosensors:**

**Table S2** Detailed oligonucleotide information used in this assay.

| Name | Sequence (5' to 3') |
|---|---|
| miR-155 | |
| *C*-indicator sequence | /5ThioMC6-D/UUAAUGCUAAU/iCy3/UGUGAUAGGGG |
| *C*-capture sequence | /5ThioMC6-D/CCCCUAUCACAAUUAGCAUUAA |
| *C*-standard sequence | UUAAUGCUAAUUGUGAUAGGGG |
| miR-155A | TTAATGCTAATTGTGATAGGTG |
| miR-155B | TTCATGCTAATTGTGATAGCGG |
| miR-155C | TCAATGCTAAGTGTGATAGGGA |
| miR-25 | |
| *N*-indicator sequence | /5ThioMC6-D/CAUUGCACUUG/iCy5/UCUCGGUCUGA |
| *N*-capture sequence | /5ThioMC6-D/UCAGACCGAGACAAGUGCAAUG |
| *N*-standard sequence | CAUUGCACUUGUCUCGGUCUGA |
| miR-25A | CATTGCACTTCTCTCGGTCTGA |
| miR-25B | CATTACACTTGTCTCGCTCTGA |
| miR-25C | CGTTGCACTTATCTCGGTCTCA |

All HPLC-purified oligonucleotides were custom-made by Integrated DNA Technologies, Inc. (IDT, Inc.). All DNA/RNA stock solutions were kept at -20 °C.

**Supporting information 4. Nanosensor synthesis:**

The synthesis route of silver-based nanosensor mainly include two parts: raw silver nanoparticle (AgNP) fabrication and nucleic acid functionalization for miRNA measurement. In the first step, AgNPs are first fabricated using a citrate mediated reduction reaction.[5] Briefly, $AgNO_3$ (36 mg) is dissolved in 200 mL of water by continuous stirring. Then, 4 mL of 1% (w/v) trisodium citrate is added to the solution. The mixture is boiled with stirring for ~1 hour and then cools to 25 °C (room temperature). In the second step, to fabricate nucleic acid-functionalized AgNPs, the paired capturer and indicator are fabricated by modification of silver nanoparticles. In brief, a cytoplasm capture sequence (C-capture sequence, 10 μM, 2 μL), which has a complementary strand to the target miRNA, is mixed with AgNPs (18 μL) in an aqueous solution to fabricate cytoplasm-miRNA nanosensors. The same procedure is applied to prepare nucleus-miRNA nanosensors. A nucleus capture sequence (N-capture sequence 10 μM, 2 μL), which has a fluorophore-labeled strand, is mixed with AgNPs (18 μL) in an aqueous solution to fabricate nucleus-miRNA nanosensors. After a 2-hour reaction at room temperature, the supernatant is discarded by centrifugation at 6000 rpm for 5 min. The sediments, consisting of nanosensors, are resuspended in 20 μL of water and stored at 4 °C. In experiment, the obtained capture nanosensor and indicator nanosensor solutions were diluted 100 times for further experiment.

For comparison, gold-based nanosensors were fabricated. The synthesis route was shown in Fig. S2, involved two main steps: the preparation of gold nanoparticles (AuNPs) and the preparation of nucleic acid-modified AuNPs. AuNPs were first prepared from chloroauric acid ($HAuCl_4$, Sigma-Aldrich, USA) through citrate-mediated (Sigma-Aldrich, USA) reduction according to a common method.[6] Briefly, 100 mL of 1 mM $HAuCl_4$ solution was boiled under continuous stirring. Then, 10 mL of 38.8 mM trisodium citrate solution was added rapidly. The mixed solution was heated for another 8 min, the color changed to purple, and the solution was then cooled to room temperature for further use. The procedures for nucleic acid modification on the surface of AuNPs were the same as those for the silver-based nanosensors except that the AgNPs were replaced by AuNPs. The sensor sequence is attached in Table S2.

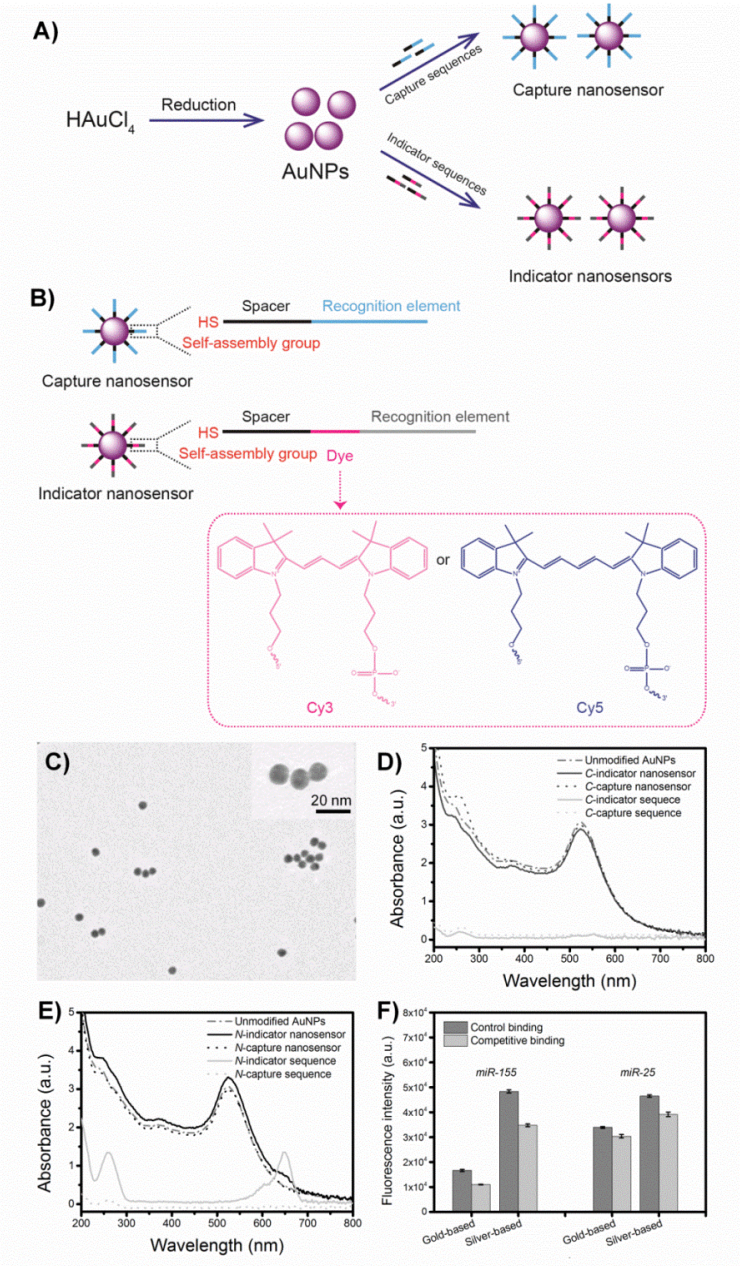


**Figure S2** Fabrication and characterization of gold-based nanosensors for nucleocytoplasmic miRNA screening. (A) Schematic of the synthesis route of unmodified AuNPs, capture nanosensors and indicator nanosensors. (B) Schematic of the capture sequence and indicator sequence attached to each gold nanoparticle. (C) Transmission electron microscopy (TEM) images of AuNPs, and the inset image shows that the diameter of the AuNP core is ~13 nm. (D, E) UV-Visible absorption spectra of unmodified AuNPs, gold-based capture nanosensors, gold-based indicator nanosensors, and the capture sequences and indicator sequences for miR-155 and miR-25, respectively. (F) Changes in the fluorescence intensity of two hybridization reactions for miR-155 and miR-25 determination in standard solutions using silver-based and gold-based nanosensors. The error bars are based on standard deviations of three parallel measurements.

**Supporting information 5. Sensing mechanism based on electromagnetic resonance:**

The sensing mechanism of nanoplasmon-enhancement is dependent on fluorescence enhancement by electromagnetic resonance. In this study, AgNP fluorescence enhancement technology is conducted to measure the target miRNA concentrations. Instead on quenching fluorescence signals, if the distance between RNA dye and AgNP metal surface is ~2-10 nm, the electrical resonance occurs, showing high fluorescence intensity. Unlike the RNA dye fluorescence quenching on metal surface in a short distance (within ~2 nm), when the distance between dye and AgNP is kept being a certain distance (~2-10 nm), the electromagnetic resonance would be triggered, showing enhanced high fluorescence intensity. This fluorescence enhancement is determined by the distance between dye and AgNP.[7]

To fabricate the AgNP couples for miRNA measurement, the dye (Cy3/Cy5) is confined between two AgNPs by the indicator sequence. When assembling AgNPs to form a couple, the dye is trapped in the middle. The distance between AgNP and dye is 3~4 nm, showing high fluorescence intensity.[8] The distance between AgNP and dye is evaluated by the sequence of RNA dye, shown in Table S2. When the target miRNA in the sample, competitive binding leads to the indicator AgNP separates from the couple. The plasmonic coupling electromagnetic field between two adjacent is affected to eliminate electromagnetic resonance for fluorescence enhancement. Based on that, the fluorescence intensity would decrease to reflect the target miRNA concentration. Compared with the conventional approach replying on RNA dyes-AgNP fluorescence quenching, the fluorescence signals from AgNP couple is well-recognized and stable.

The observed altered optical response is a combination of attenuated fluorescence and scattering as the dimers are cleaved. In this study, RNA dyes are used to fabricate AgNP dimers. The fluorescence signal irradiated by AgNP dimers is determined by the distance between dye and AgNP.[7] The distance of our fabricated AgNP dimers is ~3-4 nm. If there are no target miRNAs in a solution, the distance between RNA dye and AgNP metal surface is kept. In this case, the electromagnetic resonance between AgNP and RNA dye would be triggered, showing enhanced high fluorescence intensity

(Supporting information 5, Figure S3). Once the dimers are cleaved by the presence of target miRNA, the distance between RNA dye and AgNP metal surface is changed (to be a long distance). Accordingly, the electrical resonance disappears, causing fluorescence signal decrease. The level of optical signal decrease is conducted to evaluate miRNA concentration.

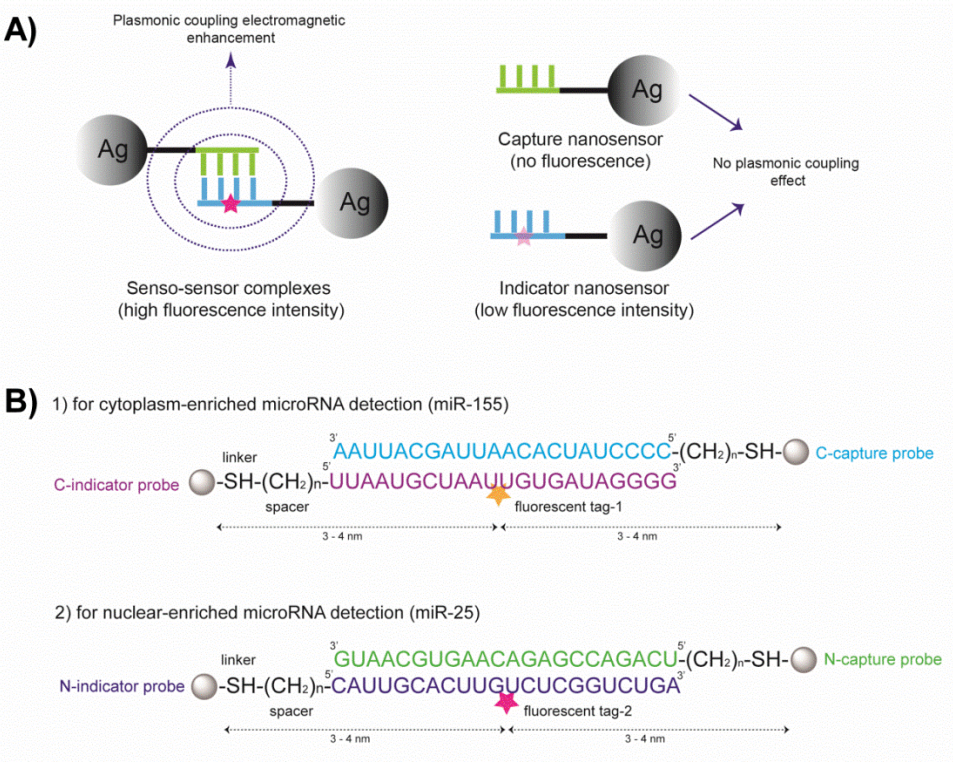


**Figure S3** (A) Schematic of plasmonic coupling electromagnetic resonance between two AgNPs for fluorescence enhancement. (B) The details of sensor design (AgNP couple, sequence on AgNP surface and RNA dye) to measure miR-155 and miR-25, respectively.

**Supporting information 6. Single-cell nucleocytoplasmic screening:**

After incubation of cells and probe solutions for 2 hours at 37 °C, the droplets were injected into a flow channel on the chip and monitored by a photomultiplier (PMT) sensor for screening the fluorescence signal. The flow rates of droplets and spacing oil were set as 3 μL/min and 10 μL/min, respectively. The fluorescence signals were rapidly collected by three PMTs, the blue channel monitored signals at a wavelength of 460 nm to identify cells, and the green channel detected signals at a wavelength of 568 nm to recognize the cytoplasmic indicator miR-155. The red channel measured signals at a wavelength of 668 nm to identify nuclear indicator miR-25. The fluorescence signals collected from PMTs were converted to digital signals (MATLAB) for fast real-time computational analysis. The fluorescent intensity distributions of the MCF-7 cell line and the droplets without cells are shown in Fig. S4 below. The concentrations of miR-155 and miR-25 in cells were calculated using the linear relationship shown in Fig. 4F (y=0.17087x-0.07998, $r^2$=0.99) and Fig. 4H (y=0.14724x-0.01582, $r^2$=0.99), respectively. The estimated concentrations of two miRNAs were shown in Fig. 5F.

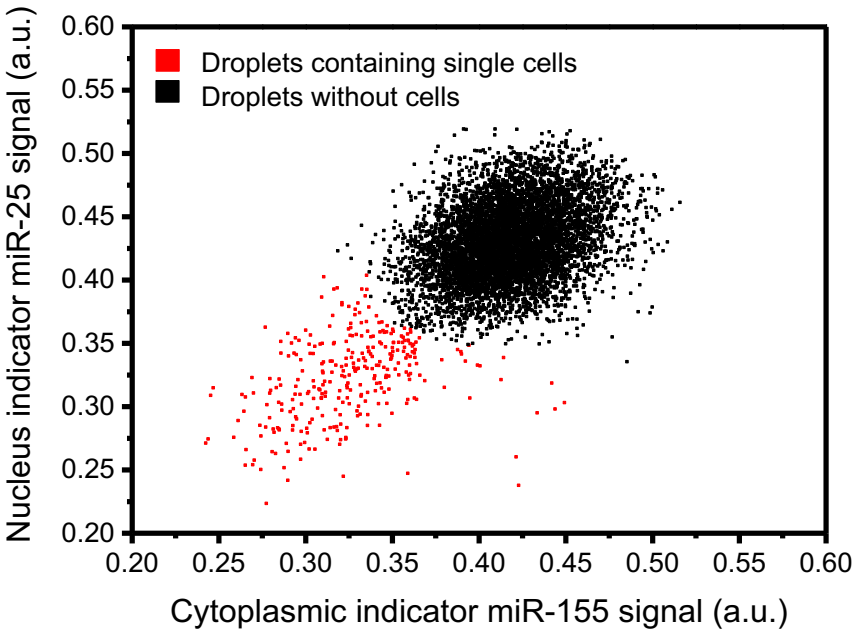


**Figure S4** Plots showing the fluorescence intensity distribution of the MCF-7 cell line. Each plot represents a single MCF-7 cell.

**References:**


1. R. P. Aaronson, G. Blobel, *Proc. Natl. Acad. Sci. USA*, 1975, **72**, 1007-1011.
2. R. Berezney, D. S. Coffey, *J. Cell Biol.*, 1977, **73**, 616-637.
3. B. J. Dodgson, A. Mazouchi, D. W. Wegman, et al. *Anal. Chem.*, 2012, **84**, 5470-5474.
4. X. F. Gao, H. Xu, M. Baloda, et al. *Biosen. Bioelectron.*, 2014, **54**, 578-584.
5. P. C. Lee, D. Meisel, *J. Phys. Chem.*, 1982, **86**, 3391-3395.
6. Y. J. Liao, Y. C. Shiang, C. C. Huang, et al, *Langmuir*, 2012, **28**, 8944-8951.
7. B. J. Yang, N. Lu, D. P. Qi, et al. *Small*, 2010, **6**, 1038-1043.
8. Q. Zhang, J. Liu, Y. R. Dong, et al. *ACS Applied Nano Materials*, 2019, **2**, 3960-3970.